Dynamic Docking of Cytochrome b 5 with Myoglobin and α-Hemoglobin: Heme-Neutralization "Squares" and the Binding of Electron-Transfer-Reactive Configurations

ARTICLE *in* JOURNAL OF THE AMERICAN CHEMICAL SOCIETY · MAY 2007

Impact Factor: 12.11 · DOI: 10.1021/ja067598g · Source: PubMed

6 AUTHORS, INCLUDING:

Korin E Wheeler
Santa Clara University
13 PUBLICATIONS **262** CITATIONS

SEE PROFILE

Judith Nocek
Northwestern University
56 PUBLICATIONS **1,436** CITATIONS

SEE PROFILE

Liliya A Yatsunyk
Swarthmore College
37 PUBLICATIONS **1,071** CITATIONS

SEE PROFILE

J|A|C|S
ARTICLES
Published on Web 03/08/2007

Dynamic Docking of Cytochrome b_5 with Myoglobin and α-Hemoglobin: Heme-Neutralization "Squares" and the Binding of Electron-Transfer-Reactive Configurations

Korin E. Wheeler, Judith M. Nocek, Deborah A. Cull, Liliya A. Yatsunyk, Amy C. Rosenzweig, and Brian M. Hoffman*

Contribution from the Department of Chemistry and Department of Biochemistry, Molecular Biology and Cell Biology, Northwestern University, 2145 North Sheridan Road, Evanston, Illinois 60208

Received October 24, 2006; E-mail: bmh@northwestern.edu

Abstract: Intracomplex electron transfer (ET) occurs most often in intrinsically transient, low affinity complexes. As a result, the means by which adequate specificity and reactivity are obtained to support effective ET is still poorly understood. We report here on two such ET complexes: cytochrome b_5 (cyt b_5) in reaction with its physiological partners, myoglobin (Mb) and hemoglobin (Hb). These complexes obey the Dynamic Docking (DD) paradigm: a large ensemble of weakly bound protein−protein configurations contribute to binding in the rapid-exchange limit, but only a few are ET-active. We report the ionic-strength dependence of the second-order rate constant, k_2, for photoinitiated ET from within all four combinations of heme-neutralized Zn deuteroporphyrin-substituted Mb/αHb undergoing ET with cyt b_5, the four "corners" of a "heme-neutralization square". These experiments provide insights into the relative importance of both global and local electrostatic contributions to the binding of reactive configurations, which are too few to be observed directly. To interpret the variations of k_2 arising from heme neutralization, we have developed a procedure by which comparisons of the ET rate constants for a heme-neutralization square permit us to decompose the free energy of reactive binding into individual *local* electrostatic contributions associated with interactions between (*i*) the propionates of the two hemes and (*ii*) the heme of each protein with the polypeptide of its partner. Most notably, we find the contribution from the repulsion between propionates of partner hemes to the reactive binding free energy to be surprisingly small, ΔG(Hb) $\sim +1$ kcal/mol at ambient temperature, 18 mM ionic strength, and we speculate about possible causes of this observation. To confirm the fundamental assumption of these studies, that the structure of a heme-neutralized protein is unaltered either by substitution of Zn or by heme neutralization, we have obtained the X-ray structure of ZnMb prepared with the porphyrin dimethyl ester and find it to be nearly isostructural with the native protein.

Most interprotein electron transfer (ET) complexes are intrinsically transient, with low affinities and short lifetimes.[1,2] This is desirable when high turnover is needed to sustain a continuous ET "current"[3,4] but an impediment to structure/function studies. As a further complication, many ET proteins are components of an ET chain and must be reactive toward two partners, a donor and an acceptor. As a result, the means by which ET proteins achieve the paradoxical requirements of low affinity for partners, yet adequate specificity and ET reactivity, are still poorly understood.

We study two such complexes involving cytochrome b_5 (cyt b_5) and its physiological ET partners: myoglobin (Mb), which stores and transports O_2 within muscles, and its tetrameric cousin, hemoglobin (Hb), the O_2 transporter in erythrocytes. Both "globins" bind O_2 in the reduced (Fe^{2+}) state but, under physiological conditions, can become oxidized to the inactive Fe^{3+}Mb/Hb state. A soluble form of cyt b_5 is known to reduce Fe^{3+}Hb back to the active Fe^{2+}Hb via interprotein ET, and an analogous reaction is thought to occur between Mb and cyt b_5: $Fe^{3+}Mb/Hb + Fe^{2+}cyt\ b_5 \rightarrow Fe^{2+}Mb/Hb + Fe^{3+}cyt\ b_5$.[5−7] These ET partners are known to bind cyt b_5 weakly ($K_a \sim 10^3\ M^{-1}$ for Mb[8,9] and $\sim 10^4\ M^{-1}$for Hb[10]), and it is easy to see how tight binding between cyt b_5 and Mb/Hb would hinder the reductive repair role of cyt b_5.

Recent studies of ET within the [Mb, cyt b_5] complex carried out by monitoring the photoinitiated ET involving Zn-substituted Mb provided the key insight that weakly binding ET partners

(1) Bendall, D. S. *Protein Electron Transfer*; BIOS Scientific Publishers: Oxford, 1996.
(2) Mathews, F. S.; Mauk, A. G.; Moore, G. R. *Front. Mol. Biol.* **2000**, *31*, 60−101.
(3) Crowley, P. B.; Ubbink, M. *Acc. Chem. Res.* **2003**, *36*, 723−730.
(4) Crowley, P. B.; Carrondo, M. A. *Proteins: Struct., Funct., Bioinf.* **2004**, *55*, 603−612.
(5) Hultquist, D. E.; Passon, P. G. *Nat. New Biol.* **1971**, *229*, 252−254.
(6) Hagler, L.; Coppes, R. I., Jr.; Herman, R. H. *J. Biol. Chem.* **1979**, *254*, 6505−6514.
(7) Goto-Tamura, R.; Takesue, Y.; Takesue, S. *Biochim. Biophys. Acta* **1976**, *423*, 293−302.
(8) Liang, Z.-X.; Jiang, M.; Ning, Q.; Hoffman, B. M. *JBIC, J. Biol. Inorg. Chem.* **2002**, *7*, 580−588.
(9) Liang, Z.-X.; Nocek, J.; Huang, K.; Hayes, R. T.; Kurnikov, I. V.; Beratan, D. N.; Hoffman, B. M. *J. Am. Chem. Soc.* **2002**, *124*, 6849−6859.
(10) Naito, N.; Huang, H.; Sturgess, W.; Nocek, J. M.; Hoffman, B. M. *J. Am. Chem. Soc.* **1998**, *120*, 11256−11262.

10.1021/ja067598g CCC: $37.00

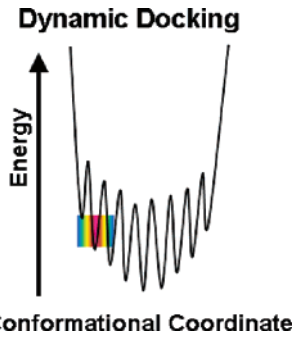

Figure 1. Schematic of the "dynamic docking" energy landscape.

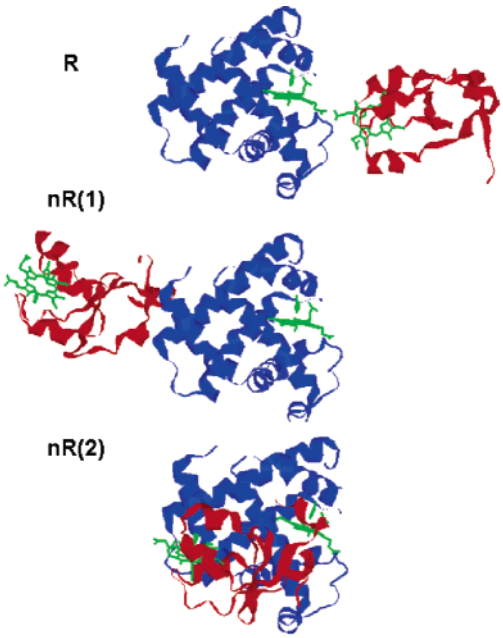

Figure 2. One representative reactive, heme-propionate-proximate configuration (top) and two representative nonreactive configurations (below) of [Mb, cyt b_5]. Structures are sampled from a MacroDox simulation.

can function *without* a simple correlation between binding and reactivity.[8,9,11−13] Such complexes operate on a "Dynamic Docking" (DD) energy/reactivity landscape (Figure 1) with multiple bound minima but few reactive configurations, and these may not include the most stable ones. Since the formalization of the DD model, it has been suggested that the cyt b_5/cyt *c* complex also may operate according to the DD paradigm;[14] in the present work we add the [Hb, cyt b_5] complex to the suite of ET partners that operate this way.

According to this paradigm, each configuration within the ensemble of protein−protein configurations has its own characteristic ET rate constant, k_{et}^{i}, its own microscopic binding free energy (ΔG_i), and binding constant, $K_a^i = \exp[-\Delta G_i/kT]$.[11] In a limiting DD model, most conformers have roughly

Scheme 1

Mb/αHb	cyt b_5 Acid	cyt b_5 Ester
Acid	AA	AE
Ester	EA	EE

comparable binding constants; none bind with exceptional affinity. The overall (thermodynamic) binding constant and second-order ET rate constants each then are the sum of the contributions from all binding configurations,

$$K = \Sigma K_a^i \qquad k_2 = \Sigma k_2^i = \Sigma k_{et}^i K_a^i \tag{1}$$

and both can be partitioned into sums over the n^R reactive conformers and N^{nR} nonreactive ones.

$$K = \Sigma K_i^R + \Sigma K_j^{nR} \qquad k_2 = \Sigma k_i^R K_i^R + \Sigma k_j^{nR} K_j^{nR} \tag{2}$$

ET PATHWAYS calculations show that the reactive configurations of the Mb/Hb−cyt b_5 complex must have one or more propionates of the partner hemes in close proximity,[11] which severely limits the possible geometries for a reactive complex, and hence $n^R \ll N^{nR}$. This is illustrated in Figure 2, which compares a sample reactive conformation found in a Brownian Dynamics (BD) simulation with two examples of nonreactive conformations. As a result, the majority of nonreactive conformers necessarily control the overall binding, while the observed second-order rate constant necessarily is controlled by the minority reactive conformers. Consequently, eq 2 can be simplified,

$$K \approx \Sigma K_j^{nR} \equiv N^{nR} K^{nR} \qquad k_2 \approx \Sigma k_i^R K_i^R \equiv n^R k^R K^R \tag{3}$$

where we define average binding constants for the reactive and nonreactive conformations and an average rate constant for the reactive ones. These equations show that the DD reactivity and binding are *"decoupled"*. While the nonreactive majority of protein−protein configurations dominate binding, the ET rate constant reflects the binding and reactivity of the small subset of reactive, "heme-propionate-proximate" conformations. This landscape thus introduces a kind of "phase-space control" of reactivity.

In fact, the DD model was developed to describe such decoupling observed during the study of ET between cyt b_5 and zinc-substituted Mb[8,9,11,12] and Hb[10,18] (ZnMb, ZnHb) reconstituted with charge-neutralized hemes. These studies involve the **AA** and **EA** corners of the charge-neutralization "square" of Scheme 1, where **A** designates a protein whose incorporated porphyrin has the native propionic acid side chains and **E** designates one with the dimethyl ester derivative. Elimination of the two negative charges on the heme propionates of Mb/Hb by esterification or amidation increased the bimolecular rate constant k_2 by as much as 2 orders of magnitude, yet the thermodynamic binding constants, as measured by ITC and

(11) Liang, Z.-X.; Kurnikov, I. V.; Nocek, J. M.; Mauk, A. G.; Beratan, D. N.; Hoffman, B. M. *J. Am. Chem. Soc.* **2004**, *126*, 2785−2798.
(12) Liang, Z.-X.; Nocek, J. M.; Kurnikov, I. V.; Beratan, D. N.; Hoffman, B. M. *J. Am. Chem. Soc.* **2000**, *122*, 3552−3553.
(13) Worrall, J. A. R.; Liu, Y.; Crowley, P. B.; Nocek, J.; Hoffman, B. M.; Ubbink, M. *Biochemistry* **2002**, *41*, 11721−11730.
(14) Ren, Y.; Wang, W.-H.; Wang, Y.-H.; Case, M.; Qian, W.; McLendon, G.; Huang, Z.-X. *Biochemistry* **2004**, *43*, 3527−3536.
(15) Naito, A.; Hui, H. L.; Noble, R. W.; Hoffman, B. M. *Biochemistry* **2001**, *40*, 2060−2065.
(16) Carter, P. J.; Winter, G.; Wilkinson, A. J.; Fersht, A. R. *Cell (Cambridge, MA, United States)* **1984**, *38*, 835−840.
(17) Selzer, T.; Albeck, S.; Schreiber, G. *Nat. Struct. Biol.* **2000**, *7*, 537−541.
(18) Tetreault, M.; Rongey, S. H.; Feher, G.; Okamura, M. Y. *Biochemistry* **2001**, *40*, 8452−8462.

NMR, were nearly unchanged.[12] Extension of these studies to Mb surface mutants further demonstrated that reactivity in this complex is controlled by the electrostatic contribution to the binding free energy of the reactive conformations (K_i^R) in agreement with eq 3.[11] In short they showed that it is possible to use measurements of ET rate constants (k_2) to probe the reactive conformations of the complex which are too few and too little populated to influence the thermodynamic binding constant *or* to be observed directly with spectroscopic or structural tools.

We herein extend heme neutralization to all four corners of the neutralization squares for Mb/αHb undergoing ET with cyt b_5 (Scheme 1) and report measurements of the ionic-strength dependence of k_2 for ET at each corner. We begin by confirming the fundamental assumption of these studies and of eqs 1−3 that the structure of a heme-neutralized protein is unaltered by heme neutralization, through determination of the X-ray structure of the dimethyl ester derivatives of ZnMb (ZnMb-dme). With this foundation, we report the ionic-strength dependence of k_2 for ET within all four corners of the neutralization square. We have simplified the ET kinetics of Hb by using monomeric αHb as a model for the tetrameric Hb reactivity, a procedure which is validated by previous work that shows αHb as a monomer gives the same rate constants as it does within the tetramer.[10,15]

The rate constants within a square are treated with an analysis procedure that allows us to decompose the free energy of reactive binding into individual *local* electrostatic contributions. The approach parallels and extends the double mutant cycle protocol that was introduced by Carter et al.[16] and is being elegantly applied to non-ET complexes by Schreiber and co-workers[17] and to interprotein ET by Okamura and co-workers.[18] Our approach yields values for the reactive-binding free energies associated with interactions between (*i*) the propionates of the two hemes and (*ii*) the heme of each protein with the polypeptide of its partner. These experiments provide insights into the importance of both global and local electrostatics on the formation of ET-active complexes.

Materials and Methods

Materials. Plasmids for expressing horse heart myoglobin (Mb), the trypsin-solubilized bovine Fe^{3+}-cytochrome b_5 and human erythrocyte Fe^{3+}-cytochrome b_5 (cyt b_5) were obtained from Professor A. Grant Mauk (University of British Columbia, Vancouver).[19,20] Human hemoglobin A_0 was isolated by anion exchange chromatography from outdated human blood obtained from a local blood bank.[21,22] The α-chains of Hb (αHb) were isolated using the chain method[21] as described by Naito et al.[15] Our experiments with Mb use a truncated form of the membrane-bound form of cyt b_5 found in bovine hepatocytes (bov); our experiments with αHb use its physiological partner, the soluble form of cyt b_5 from human erythrocytes (HE).

Preparation of Metalloporphyrin-Substituted Proteins. Ferric-protoporphyrin IX dimethylester (Fe^{3+}P-dme), Zn-deuteroporphyrin IX (ZnD), and Zn-deuteroporphyrin IX dimethylester (ZnD-dme) were purchased from Frontier Scientific. ZnDMb and ZnDMb-dme were prepared as described previously by our lab.[8,23] ZnDαHb and ZnDαHb-dme were prepared according to procedures similar to those described by Naito for the reconstitution of apo-αHb with Zn-mesoporphyrin IX[10] and apo-Hb with ZnD-dme.[15] The procedure for extracting heme and reconstituting the apo-bov-cyt b_5 with Fe^{3+}P-dme followed the method of Mauk and co-workers.[24] We found that the same procedure worked well with HE-cyt b_5.

CD Structural and Thermal Stability Studies. CD spectra and thermal denaturation experiments were performed with a Jasco, J-715 spectrometer. Quartz cells with a 1.0 cm path length were used for all experiments. Each spectrum was recorded from 190−450 nm at a scan speed of 100 nm/min, a response time of 2 s, and a bandwidth of 1 nm, averaged over 5 scans. Measurements were carried out at pH 7.0 and low ionic strength (10 mM KPi), and samples contained ∼10 μM protein. Thermal denaturation curves were collected by increasing the temperature in 2° increments from 20 to 50 °C, with equilibrations for 2 min at each temperature before recording the ellipticity at 220 nm. Results are shown in the Supporting Information (Figure S1).

Crystallization, Data Collection, and Structure Determination of ZnDMb-dme. The purified myoglobin reconstituted with ZnD-dme was crystallized by the hanging-drop vapor diffusion method in the dark at 20 °C. Thin pink plates of approximate dimension 0.5 mm × 0.2 mm × 0.05 mm grew from a well solution of 3.3 M $(NH_4)_2SO_4$, 0.1 M sodium acetate, pH 7.0 mixed 1:2 with 12−17 mg/mL myoglobin in 3.3 M $(NH_4)_2SO_4$, 0.1 M sodium acetate, pH 7.0. For data collection, crystals were transferred to a cryosolution containing 2.0 M $(NH_4)_2SO_4$ and 27% glycerol and immediately flash-cooled in liquid nitrogen. Data were collected at 100 K at the Advanced Photon Source beamline 23ID which is operated by GM/CA-CAT.

Data were integrated using HKL2000 and scaled with SCALEPACK.[25] The crystals belong to the space group $P2_1$ ($a = 42.60$ Å, $b = 30.58$ Å, $c = 56.48$ Å, $\beta = 97.66°$) with one protein molecule per asymmetric unit. Phases were determined by molecular replacement with Phaser[26] using horse heart metmyoglobin (PDB accession code 1YMB) without the heme as a search model. The initial refinement was performed with CNS[27] and then completed with REFMAC5 from the CCP4 program suite[28] after model improvement in Coot-0.1[29] guided by $2F_o-F_c$ and F_o-F_c maps. The appropriate ZnD-dme heme library was prepared in CCP4[28] by modification of protoheme IX, followed by regularization and parametrization. ZnD-dme heme is nonsymmetrical and can enter the heme pocket of Mb in two orientations, as shown originally by NMR studies.[30] The two orientations were observed in the electron density maps and were modeled as two components (A and B) with occupancies of 0.6 and 0.4, respectively. The two orientations are roughly related by a 2-fold rotation about the axis that passes through the meso-α and meso-γ carbon atoms. The modeled hemes are shifted relative to each other by 0.42 Å (measured between the two zinc atoms). Comparisons in the Results and Discussion sections are made using the A component of the heme unless otherwise specified.

The side chain of Asn 12 was visible in two conformations, which were modeled with occupancies of 0.4 and 0.6. The final model contains 153 residues, one SO_4^{2-} ion, one ZnD-dme heme modeled in two positions, and 94 water molecules. Refinement statistics are given in

(19) Funk, W. D.; Lo, T. P.; Mauk, M. R.; Brayer, G. D.; MacGillivray, R. T. A.; Mauk, A. G. *Biochemistry* **1990**, *29*, 5500−5508.
(20) Lloyd, E.; Ferrer, J. C.; Funk, W. D.; Mauk, M. R.; Mauk, A. G. *Biochemistry* **1994**, *33*, 11432−11437.
(21) Williams, R. C.; Tsay, K. *Anal. Biochem.* **1973**, *54*, 137−145.
(22) Scholler, D. M.; Wang, M.-Y. R.; Hoffman, B. M. In *Methods in Enzymology, Part C*; Fleischer, S., Packer, L., Eds.; Academic Press, Inc.: New York, 1978; Vol. 52, pp 487−493.
(23) Nocek, J. M.; Sishta, B. P.; Cameron, J. C.; Mauk, A. G.; Hoffman, B. M. *J. Am. Chem. Soc.* **1997**, *119*, 2146−2155.
(24) Reid, L. S.; Mauk, M. R.; Mauk, A. G. *J. Am. Chem. Soc.* **1984**, *106*, 2182−2185.
(25) Otwinowski, Z.; Minor, W. In *Methods in Enzymology*; Carter, C. W. J., Sweet, R. M., Eds.; Academic Press, 1997; Vol. 276, pp 307−326.
(26) Storoni, L. C.; McCoy, A. J.; Read, R. J. *Acta Crystallogr., Sect. D* **2004**, *60*, 423−438.
(27) Brünger, A. T.; Adams, P. D.; Clore, G. M.; Delano, W. L.; Gros, P.; Grosse-Kunstleve, R. W.; Jiang, J.-S.; Kuszewski, J.; Nilges, N.; Pannu, N. S.; Read, R. J.; Rice, L. M.; Simonson, T.; Warren, G. L. *Acta Crystallogr., Sect. D* **1998**, *54*, 905−921.
(28) *CCP4*; *Acta Crystallogr., Sect. D* **1994**, *D50*, 760−763.
(29) Emsley, P.; Cowtan, K. *Acta Crystallogr., Sect. D* **2004**, *60*, 2126−2132.
(30) McLachlan, S. J.; La Mar, G. N.; Burns, P. D.; Smith, K. M.; Langry, K. C. *Biochim. Biophys. Acta* **1986**, *874*, 274−284.

Table S1. A Ramachandran analysis in PROCHECK[31] shows that 92.5% of the residues are within the most favorable regions with the remainder in additionally allowed regions. Root-mean-square deviations (rmsds) for superpositions were calculated in LSQMAN[32] using the brute_force function (fragment length = 10, fragment function = 2). The refined coordinates have been deposited in the Protein Data Bank (PDB code 2IN4).

Kinetic Measurements. Proteins were exchanged into working phosphate buffers using Centricon microconcentrators (Amicon). Buffers at higher ionic strengths were made with 10 mM KPi, adjusted to the desired ionic strength with NaCl. Samples for ET studies were prepared in the dark under a N_2 atmosphere as described.[23] Glucose oxidase/catalase enzymatic O_2 scavengers were found to interfere with the reactions of [Mb-dme/αHb-dme, cyt b_5] and were not employed. Protein concentrations were determined spectrophotometrically using a diode array spectrophotometer (Agilent 8453): $\epsilon_{414\ nm}$(ZnDMb) = ϵ_{414nm}(ZnDMb-dme) = 360.8 mM^{-1} cm^{-1};[11] ϵ_{414nm}(ZnDαHb) = ϵ_{414nm}-(ZnDαHb-dme) = 280 mM^{-1} cm^{-1};[10] ϵ_{414nm}(Fe^{3+}cyt b_5-bov) = ϵ_{414nm}(Fe^{3+}cyt b_5-bov-dme) = 117 mM^{-1} cm^{-1};[33] ϵ_{414nm}(Fe^{3+}cytb_5-HE) = ϵ_{414nm}(Fe^{3+}cytb_5-HE-dme) = 122 mM^{-1} cm^{-1}.[20]

Flash photolysis measurements were performed with an LKS60 photolysis unit (Applied Photophysics, Surrey, UK) equipped with a pulsed Xe arc lamp (75 W). Samples were excited with pulses from the second harmonic (532 nm, >60 mJ, 10 ns) from a Q-switched Nd:YAG laser (Continuum). Mb/αHb triplet decays were recorded at 475 nm. Intermediates formed during ET for the [αHb, cytb_5] and [Mb, cyt b_5] "squares" were monitored at the ~561 nm isosbestic point for the triplet decay reaction (not shown). The fitting procedures are discussed in the Supporting Information. Bimolecular rate constants measured at pH 7 have uncertainties of ±10%, as does the product of the correlated parameters, K_a and k_q measured at pH 6.5.

Brownian Dynamics Simulations. The MacroDox program, developed by Northrup and co-workers,[34,35] was used to compute the total charge (q_{net}), to determine dipole moments,[36] and to perform BD simulations. The Linux version of the program was kindly provided by Professor Kathyrn Thomasson.

Coordinates derived from X-ray crystal structures were used as input for computing the electrostatic properties of each protein: horse metmyoglobin (1ymb.pdb);[37] the α-chains from the T-state structure of human deoxyhemoglobin (1dxu.pdb);[38] and the tryptic fragment of bovine ferri-cytochrome b_5 (1cyo.pdb).[39] As there are only minor differences between bov-cyt b_5 and HE-cyt b_5 and there is no published crystal structure for HE-b_5, we used the bovine structure for the docking calculations with all Mb/αHb complexes.[40]

Protonation states of the titratable residues were assigned by MacroDox using the Tanford−Kirkwood calculation.[41,42] Each residue was assigned a net charge based on its environment (pH = 7.0; μ = 18.0 mM; temperature = 293 K). For calculations with a heme-neutralized protein, the carboxylate oxygens of the heme propionates were treated as uncharged atoms and the slight differences in molecular weight were ignored. All computations shown here were done with 10 000 trajectories (for details, see Supporting Information). Two alternate criteria for a successful BD trajectory were employed, as discussed in the Results section.

Results

Spectroscopic Characterization. The preparation and spectroscopic properties of ZnMb and ZnMb-dme have been previously described,[8,23] and the ZnαHb and ZnαHb-dme behave quite similarly.[10,15] These native and heme-neutralized ZnMb and ZnαHb have nearly identical optical spectra with Soret-band absorbance maxima at 414 nm and $\alpha-\beta$ bands at 542 and 575 nm (ZnαHb), 576 nm (ZnMb). The triplet-ground kinetic difference spectra of the photoexcited ZnMb, ZnMb-dme, αZnHb, and αZnHb-dme were measured as the zero-time absorbance difference following flash photolysis and also are identical within error.[40]

Recombinant HE- and bov-cyt b_5 proteins were prepared as described.[19,20,33] The Fe^{3+}P-dme derivatives were prepared by removing the hemes and reconstituting the apoprotein with Fe^{3+}P-dme following the method of Mauk and co-workers.[24] Cyt b_5 and cyt b_5-dme have virtually identical UV−vis spectra, with a Soret maximum at 414 nm and α- and β-bands at 532 and 562 nm, respectively. The room-temperature CD spectra (see Supporting Information, Figure S1) of the native and heme-neutralized ZnMb, ZnαHb, and bov- and HE-cyt b_5 at 20 °C show no evidence of structural changes caused by the heme neutralization.

X-ray Structure of ZnMb-dme. This is the first reported structure of a Zn-substituted Mb or a heme-neutralized protein. The crystallographic data indicate that neither substitution of iron with zinc nor heme neutralization affect the overall Mb fold (Figure 3). Likewise, the finding of two heme conformers parallels that for the native Mb.[30] The rmsd's for the Cα atoms of ZnMb-dme superimposed on the Mb from the same species (horse heart Fe^{3+}Mb, PDB accession code 1YMB[37]) or on the same oxidation state of the central metal ion (sperm whale Fe^{2+}-Mb, 88% sequence homology, PDB accession code 1A6N[43]) are 0.728 and 0.456 Å, respectively. The heme environment is also quite similar in all three structures. The heme is five-coordinate in ZnMb-dme and the Fe^{2+}Mb 1A6N,[44] whereas an axial water ligand is present in the Fe^{3+}Mb 1YMB, with an Fe−O distance of 2.29 Å. There is a distant water molecule in the heme binding pocket in 1A6N with an Fe−O distance of 3.53 Å; there is no difference in density attributable to a water molecule in the heme pocket of our structure. In all three structures, the proximal His 93 is coordinated to the metal ion by its ϵ nitrogen with Fe−N distances of 2.17 Å, 2.14 Å, and 2.26 Å for ZnMb-dme, 1A6N, and 1YMB, respectively. The orientation of His 93 is stabilized by hydrogen bonds to the side chain O of Ser 92 and main chain carbonyl O of Leu 89 (3.05, 2.98 Å in ZnMb-dme; 2.95, 2.86 Å in 1A6N; and 3.01, 3.01 Å in 1YMB). The distal histidine, His 64, is 4.42 Å away from Zn(II) (measured from the ϵ nitrogen) in ZnMb-dme. This histidine adopts slightly different positions in 1A6N and 1YMB, probably due to the presence of a water molecule in the heme pocket, but the Fe−N distance does not change significantly (4.40 Å for 1A6N and 4.33 Å for 1YMB).

(31) Laskowski, R. A.; MacArthur, M. W.; Moss, D. S.; Thornton, J. M. *J. Appl. Crystallogr.* **1993**, *26*, 283−291.
(32) Kleywegt, G. J.; Jones, T. A. In *From first map to final model*; Bailey S, H., R., Waller, D., Eds.; SERC Daresbury Laboratory: Warrington, U.K., 1994; pp 59−66.
(33) Ozols, J.; Strittmatter, P. *J. Biol. Chem.* **1964**, *239*, 1018−1023.
(34) Northrup, S. H.; Boles, J. O.; Reynolds, J. C. L. *Science* **1988**, *241*, 67−70.
(35) Northrup, S. H.; Thomasson, K. A.; Miller, C. M.; Barker, P. D.; Eltis, L. D.; Guillemette, J. G.; Inglis, S. C.; Mauk, A. G. *Biochemistry* **1993**, *32*, 6613−6623.
(36) Koppenol, W. H.; Margoliash, E. *J. Biol. Chem.* **1982**, *257*, 4426−4437.
(37) Evans, S. V.; Brayer, G. D. *J. Mol. Biol.* **1990**, *213*, 885−897.
(38) Kavanaugh, J. S.; Rogers, P. H.; Arnone, A. *Biochemistry* **1992**, *31*, 8640−8647.
(39) Durley, R. C. E.; Mathews, F. S. *Acta Crystallogr.* **1996**, *D52*, 65−76.
(40) Naito, N. R. PhD Thesis; Northwestern University: Evanston, IL, 1999.
(41) Matthew, J. B. *Annu. Rev. Biophys. Biophys. Chem.* **1985**, *14*, 387−417.
(42) Tanford, C.; Kirkwood, J. G. *J. Am. Chem. Soc.* **1957**, *79*, 5333−5339.
(43) Vojtechovsky, J.; Chu, K.; Berendzen, J.; Sweet, R. M.; Schlichting, I. *Biophys. J.* **1999**, *77*, 2153−2174.
(44) The Zn of Heme A Zn is 0.280 Å out of the mean N4 plane, while that of Heme B is 0.347 Å; this compares with 0.39 Å for the Fe(II) of 1A6N.

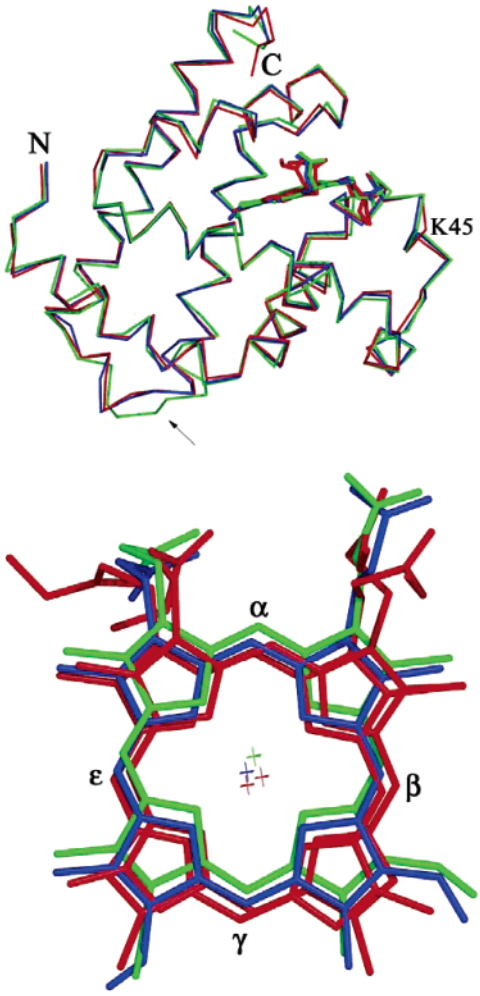

Figure 3. (Upper) Superposition of the ZnMb-dme (red) with Mb 1A6N (blue) and 1YMB (green) polypeptides. (Lower) Superposition of the hemes from the three structures. Two red hemes correspond to the two heme orientations of ZnMb-dme. The loop spanning residues 115−123 is indicated with an arrow.

The deviations in the loop spanning residues 115−123 (1YMB) and at the C-terminus (Figure 3) are probably due to crystal packing. There are, however, some small, subtle differences that can be attributed to the neutralization of the heme. *First*, the heme is buried slightly deeper in the protein by ∼0.4 Å and ∼0.8 Å (measured between meso-γ carbon atoms) as compared with 1A6N and 1YMB, respectively (Figure 3B). *Second*, positively charged residue 45 (Lys in horse heart and Arg in sperm whale Mb) forms a salt bridge (2.90 Å in 1A6N and 2.47 Å in 1YMB) with the nearest negatively charged propionate. In ZnMb-dme, the propionate groups are neutralized precluding the formation of the salt bridge. As a result, the Cα atom of Lys 45 is shifted away from the heme pocket by 1.27 and 1.01 Å as compared to the corresponding atom in 1A6N and 1YMB, respectively (Figure 3) with its side chain turned away facing the solvent and forming a hydrogen bond with a water molecule (3.39 Å). This propionate is stabilized in ZnMb-dme by a hydrogen bond between the ester O and δN of distal His 64, 3.30 Å, that is not present in the other structures. In spite of the heme neutralization, a hydrogen bond network of the second propionate group with His 97 and Ser 92 is very similar to that in 1A6N and 1YMB. The side chain O atom of Ser 92 forms hydrogen bonds to the carbonyl O atom of the heme A conformation (2.93 Å) and the ester O atom of the heme B conformation (2.69 Å); the ϵ N of His 97 interacts with the carbonyl O atom of heme B (2.99 Å). Both Ser 92 and His 97 are located near the proposed pathway for O_2 entry and exit.[37] The fact that this hydrogen-bonding network is preserved in the protein with a neutralized heme emphasizes its importance for Mb function.

Overall, the structural data confirm the assumption[8,11,12,45] that the substitution of Fe protoporphyrin IX with ZnD-dme in Mb does not significantly alter the protein fold, heme position, or binding pocket. The NMR structure of rat cyt b_5-dme likewise showed only slight perturbations upon heme-replacement.[46] Thus, a basic hypothesis of the DD docking model is verified.

Electrostatic Properties. We used IEF to detect changes in pI upon heme modification and to compare these to calculations with the MacroDox software package, Table S2. In all instances there is an increase in pI. The pI's of the ZnMb and ZnαHb, which are slightly basic, increase by 0.7 and 0.4 pH units upon heme neutralization. The pI's of the acidic bov- and HE-cyt b_5, measured to be 4.4 and 4.8, increase by ∼0.25 pH upon heme neutralization. Although the calculated pI's are lower than the experimental by up to 0.4 pH units, the changes in pI between the native and heme-neutralized proteins are nearly equal.

As the affinity of Mb and αHb for cyt b_5 is dominated by the electrostatic interactions between the protein partners, we have used the MacroDox software package to compute the net charge and dipole moments of Mb/αHb and cyt b_5 (Table S2) and the GRASP program to visualize the electrostatic surfaces (see Supporting Information, Figure S2). The 53 charged residues of Mb (21 acidic residues and 32 basic residues) are scattered fairly evenly over the protein surface, and the result of this arrangement leaves Mb with only a small net negative charge at pH 7 ($q_{net} = -0.24$ for Mb). Although Mb and αHb have a high degree of sequence homology,[47] αHb has fewer charged residues (12 acidic and 24 basic residues) and the calculations indicate that αHb has a more positive overall charge ($q_{net} = 2.2$ at pH 7, Table S2). Because the charged residues are scattered over the surface of both ZnMb and ZnαHb, both proteins have small dipole moments: 293 D and 111 D for Mb and αHb, respectively.

In contrast, the bov- and HE-cyt b_5 are strongly acidic proteins. The two cyt b_5 species are very similar in structure and reactivity, and accordingly, as mentioned earlier, our calculations with MacroDox are only with the bov-cyt b_5 structure.[40] The distribution of the 33 charged residues of cyt b_5 is highly asymmetric: there are 17 surface acidic residues located on the "front" face near the partially exposed heme edge, and most of the 16 basic residues are positioned on the opposite face. Consequently, there is an appreciable resultant net negative charge at pH 7 ($q_{net} = -5.61$, Table S2), and this asymmetric distribution of charge gives cyt b_5 a very large dipole moment of 645 D.

Neutralization of the Mb, αHb, and cyt b_5 hemes by replacement with a dimethylester porphyrin increases the computed

(45) Liang, Z.-X. In *Chemistry*; Northwestern University: Evanston, IL, 2001.
(46) Banci, L.; Bertini, I.; Branchini, B. R.; Hajieva, P.; Spyroulias, G. A.; Turano, P. *J. Biol. Inorg. Chem.* **2001**, *6*, 490−503.
(47) Dickerson, R. E.; Geis, I. *Hemoglobin: Structure, Function, Evolution, and Pathology*; Benjamin/Cummings: Menlo Park, CA, 1983.

net charge on both Mb and αHb, by $\Delta q_{net} = +1.6$ and decreases the negative charge of cyt b_5 by Δq_{net}(cyt b_5) = +1.85.

ET Quenching in the Heme-Neutralization "Square" (Scheme 1). Photoexcitation of ZnMb and ZnαHb with the second harmonic of a Nd:YAG laser (λ_{ex} = 532 nm) produces a singlet excited state which rapidly and efficiently converts to the triplet state via intersystem crossing. Time-resolved triplet decay traces for the native and heme-neutralized ZnMb and ZnαHb are exponential with rate constants in the range 50 $s^{-1} < k_d \leq 80\ s^{-1}$: ZnMb = 50(±5) s^{-1}; ZnMb-dme = 80 (±8) s^{-1}; ZnαHb = 50 (±5) s^{-1}; and ZnαHb-dme = 70(±12) s^{-1}.[8,9,15,40] Upon addition of native or heme-neutralized cyt b_5 to a native or heme-neutralized Mb/αHb, the triplet-decay progress curves remain exponential but the decay rate constant, denoted k_{obsd}, is increased by ET quenching ($k_q = k_{obsd} - k_d$) (see Supporting Information, Figure S3). This indicates that all four combinations of native and heme-neutralized partners (Scheme 1) are in the rapid-exchange limit, as we found previously for the **AA** and **EA** complexes of both Mb and αHb with cyt b_5.[9] In all cases, the quenching was confirmed to involve ET through observation of the time-resolved absorbance spectra of the ET intermediates (data not shown).

The values of k_q for the heme-neutralized Mb and αHb in reaction with cyt b_5 are ~10^2-fold greater than those of the native acid derivative ($k_{q(EA)}/k_{q(AA)} = 92$ for Mb and 98 for αHb in 10 mM KPi, pH 7).[8,9,15,40] Surprisingly, the reaction of acid Mb/αHb with heme-neutralized cyt b_5 (the **AE** combination in Scheme 1) does *not* show an increase in quenching similar to that of the **EA** complex ($k_{q(AE)}/k_{q(AA)}$ = 1.5/0.54 for Mb/αHb, respectively). Furthermore, the rate for the **EE** complex, although greater than that for **AA**, actually is slower than the rate for the **EA** complex ($k_{q(EE)}/k_{q(AA)}$ = 38/21 for Mb/αHb, respectively).

ET Quenching at Low Ionic Strength. Quenching titrations by cyt b_5 were performed with all four combinations of Mb/αHb with cyt b_5 (Scheme 1) at low ionic strength, μ = 18 mM at pH 7 (Figure 4B, C); titrations for αHb were also performed at μ = 18 mM at pH 6.5 (Figure 4A). The single-line arrows in Figure 4 connect the **AA** curve with the titration curves resulting from the reaction when *one* of the two reacting proteins is heme-neutralized, **EA** and **AE** from Scheme 1. The double arrows connect the **AA** curve of the native protein complex to that of the doubly heme-neutralized complex, the **EE** from Scheme 1. Throughout each of the titrations, the triplet decays are exponential, indicating that the complexes are in the fast-exchange limit.

At pH 6.5, the titration profiles for the four [αHb, cyt b_5] complexes show appreciable curvature and the binding isotherms can be fit to a one-site binding equation (Table 1 and Supporting Information) to give the net binding and ET rate constants, K_a and k_q. Figure 4A overlays the titration profiles for these four complexes at pH 6.5. The rate constant and association constant for the native **AA** complex at pH 6.5 are consistent with previous findings, k_q = 3300 s^{-1} and $K_a = 7 \times 10^3\ M^{-1}$.[15,40] The influence of heme neutralization in the [αHb, cyt b_5] complex again is seen to be highly asymmetric: neutralization of αHb (**EA**) results in a sharp increase in the ET rate, whereas neutralization of cyt b_5 (**AE**) actually results in only a *slight* change in ET rate. Neutralization of both protein partners (**EE**) yields another surprising result: the bimolecular quenching rate

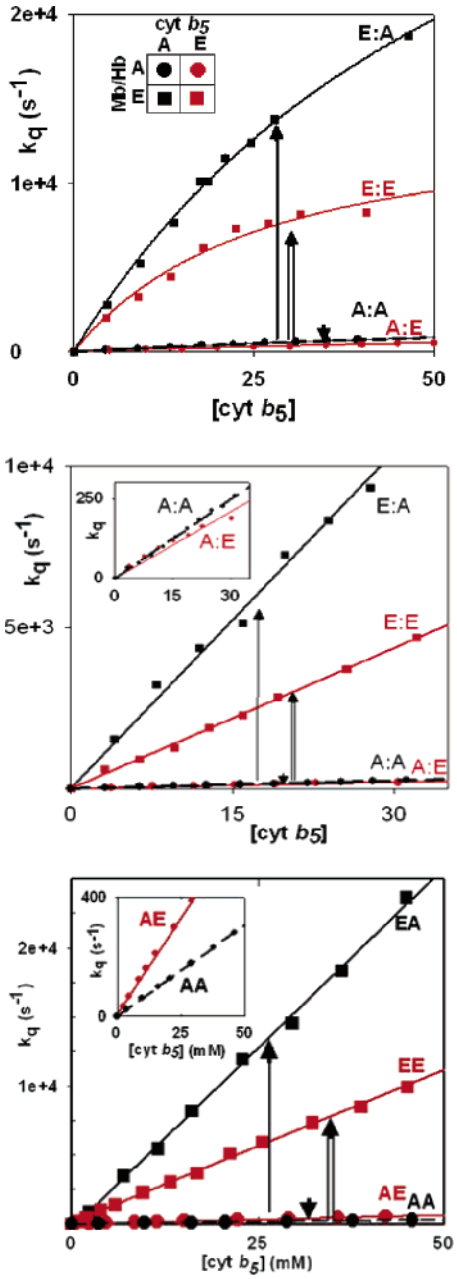

Figure 4. Triplet quenching titration curves of the neutralization "square" for the following: (Upper) αHb with cyt b_5 at pH 6.5, 10 mM; [αHb] = ~5 mM. (Middle) αHb with cyt b_5 at pH 7.0, 10 mM; [αHb] = ~5 mM. (Lower) Mb with cyt b_5 at pH 7.0, 10 mM; [Mb] = ~5 mM; T = 20 °C. **AA** titration is shown with a dashed line, for emphasis. Single arrows show change from native **AA** complex upon neutralization of the heme of one partner (either **EA** or **AE**); double arrow shows change for doubly neutralized **EE** complex.

Table 1. Binding Association (K_a), Triplet Quenching Rate (k_q), and Bimolecular Rate (k_2) Constants for the Complexes of the [αHb, cyt b_5] Reactivity "Square" at pH 6.5 10 mM KPi

		cyt b_5	
α-Hb		**A**	**E**
A	k_q (s^{-1})/10^3	3.3	3.1
	K_a (M^{-1})/10^3	7.0	4.0
E	k_q (s^{-1})/10^3	64	14
	K_a (M^{-1})/10^3	17	46

constant for the doubly modified **EE** complex is *lower* than the quenching rate constant of the singly modified **EA** ($k_{q(EE)}/k_{q(AA)}$= 4.2). Overall, double neutralization provides no ad-

Table 2. Bimolecular Rate (k_2) Constants (/10^6 M^{-1} s^{-1}) for the Complexes of the [Mb/αHb, cyt b_5] Reactivity "Square" at pH 7.0 10 mM KPi

	cyt b_5	
Mb/α-Hb	**A**	**E**
A	6.1/8.7	8.9/4.7
E	560/850	230/130

ditional enhancement in rate constant over the singly modified **EA** complex; however, the strongest binding occurs when both proteins are heme-neutralized (for **EE**, $K_a = 5 \times 10^4$ M^{-1} s^{-1}).

The ET quenching for the four [αHb, cyt b_5] complexes is pH dependent. The binding constant for these complexes decreases at pH 7, so that quenching is pseudo-first-order with the quenching constant (k_q) increasing linearly upon addition of cyt b_5;[8,15,40] the four [Mb, cyt b_5] complexes show pseudo-first-order kinetics at both pH's. The pH 7.0 titrations of all four heme-neutralized complexes of Mb/αHb with cyt b_5 are shown in Figure 4; as in Figure 4A (pH 6.5), single and double arrows are used to show the effects of single and double heme neutralizations. The slopes of these titration curves give the bimolecular quenching rate constant ($k_2 = K_a \cdot k_q$)[8,9] for the heme-neutralization squares for the [Mb, cyt b_5] and the [αHb, cyt b_5] complexes at pH 7 (Table 2).

The influence of heme neutralizations on the reactivity of both ZnMb/ZnαHb with cyt b_5 at pH 7 follow the same trends as that of αHb at pH 6.5; quenching decreases in the order $k_{2(EA)} > k_{2(EE)} > k_{2(AA)} \approx k_{2(AE)}$. As reported previously,[8,9] $k_2 = 6.1 \times 10^6$ M^{-1} s^{-1} for the **AA** complex of Mb. The αHb chains used here were reconstituted with ZnD and are quenched by cyt b_5 with $k_2 = 8 \times 10^6$ M^{-1} s^{-1}. Neutralization of Mb/αHb (**EA**) results in a dramatic increase in rates, $k_{2(EA)}/k_{2(AA)} = 9.2$ (Mb-dme) and 9.8 (αHb-dme).[9,15] Neutralization of the heme propionates on cyt b_5 (**AE**), on the other hand, causes only a small change in k_2 compared to the **AA** combination, $k_{2(AE)}/k_{2(AA)} = 1.5$ for Mb and 0.5 for αHb. For both Mb and αHb, the reactivity of **EE** is less than that of **EA** but still higher than that of the **AA** complex ($k_{2(EE)}/k_{2(AA)} = 38$ for Mb/21 for αHb). Again, double neutralization does not enhance reactivity but rather actually decreases reactivity in comparison with that of the **EA** complex.

Ionic Strength Variations. The bimolecular rate constant, k_2, at pH 7.0 was measured as a function of ionic strength (μ) for both the [Mb, cyt b_5] and the [αHb, cyt b_5] "squares" (see Supporting Information, Figure S4).[48] For both Mb and αHb at low ionic strength ($\mu = 18$ mM), the bimolecular rate constants follow the sequence, $k_{2(EA)} > k_{2(EE)} \gg k_{2(AA)} \sim k_{2(AE)}$. All rates decrease as the ionic strength is increased by additions of NaCl, as expected for electrostatic protein−protein interactions. By $\mu = 0.4$ M, all four Mb complexes have comparable rate constants, $k_2 \approx (2-4) \times 10^6$ M^{-1} s^{-1}; for αHb at $\mu = 0.4$ M, **AA** ≈ **AE** at $k_2 \approx (2-3) \times 10^6$ M^{-1} s^{-1} and **EA** ≈ **EE**, $k_2 \approx (1-2) \times 10^6$ M^{-1} s^{-1}. As expected for the complexes that have larger charge products, the rate constants for the **EA** and **EE** partners drop much more sharply, decreasing by ~10^3 at 400 mM ionic strength. Thus, at high ionic strength, differences among the rate constants of the heme-neutralization "square" are minimal; this is especially so for Mb, where rates roughly converge at a final, common value.

(48) The ionic strength dependence of the bimolecular rate constant measured for the [αHb, cyt b_5] square also was measured at pH 6.5; only the results at pH 7 are shown and discussed here. Both pH's gave similar results, with the exception that at pH 6.5 the rates were slightly faster and more dependent on ionic strength. Thus, in order to simplify the comparison with the Mb results, we have limited our discussion to ionic strength dependences at pH 7.

Table 3. Fit Parameters from the Debye−Huckel Equation, $a(Z_D \bullet Z_A)$ and log $k_{2,0}$, for the Mb and αHb Protein Complexes at pH 7

	Mb		αHb	
	a (C^2)	log($k_{2,0}$)	a (C^2)	log($k_{2,0}$)
AA	−4.67	7.16	−6.85	7.18
AE	−3.87	7.16	−6.48	7.44
EA	−29.69	11.08	−25.92	11.05
EE	−22.54	9.83	−19.15	9.78

The dependences on μ are conveniently fit by the simple Debye−Huckel model (DH), which treats the proteins as point charges interacting in a continuum with ionic strength, μ:[49,50]

$$\ln k_2(Z_D \cdot Z_A) = \ln k_{2,0}(D,A) - \frac{a(Z_D \cdot Z_A)\sqrt{\mu}}{1 + b\mu}$$

$$a(Z_D \cdot Z_A) = 2.34 Z_D \cdot Z_A$$

$$b = 0.329 R_{av} \qquad (4)$$

Here, $k_{2,0}(D,A)$, is the second-order rate constant at zero ionic strength ($\mu = 0$) for interacting species with charges Z_D, Z_A; the μ-dependent term reflects the screening of electrostatic interactions by the ionic atmosphere. R_{av} is the average of the radii of the two proteins taken as spheres; we used $R_{av} = 17.5$ Å, consistent with the sum of radii employed in the BD simulations discussed below. The parameters derived from the DH fits, $k_{2,0}$ and $a(Z_D \bullet Z_A)$, for the Mb and αHb neutralization "squares" are given in Table 3.[49,50] While $a(Z_D \bullet Z_A)$ is proportional to the charge product of the two proteins, the resulting charge product does not match those calculated by the Tanford−Kirkwood (TK) technique. As reviewed by Selzer[51] and Matthew et al.,[41] this apparent difference most likely reflects the fact that the nonuniformity of the protein charge distribution plays a major role in the electrostatic interactions between Mb/αHb and cyt b_5. However, the trends in the DH and TK charge products among members of a heme-neutralization square parallel one another.

Figure 5 shows that log k_2 for the heme-neutralized "squares" varies linearly with respect to the protein−protein charge products as computed by TK theory. The same dependence is found for the charge products determined from the parameter, $a(Z_D \bullet Z_A)$, of the DH fits (not shown), even though the two sets of charge products differ, as noted just above. The logarithmic behavior indicates that the second-order kinetics are not simply a consequence of electrostatically driven diffusion, where k_2 would be proportional to the charge product itself.[11,52] It confirms the applicability of eqs 2 and 3: k_2 is proportional to the binding constant for reactive docking, with the free energy of reactive binding dominated by electrostatic attractions.[11]

Model for Determining Electrostatic Heme Interactions. The ET rate constant for a DD protein complex written in terms of the average binding and rate constants for the small subset

(49) Zhou, J. S.; Kostic, N. M. *Biochemistry* **1993**, *32*, 4539−4546.
(50) Sokerina, E. V.; Ullmann, G. M.; Van Pouderoyen, G.; Canters, G. W.; Kostic, N. M. *JBIC, J. Biol. Inorg. Chem.* **1999**, *4*, 111−121.
(51) Selzer, T.; Schreiber, G. *J. Mol. Biol.* **1999**, *287*, 409−419.

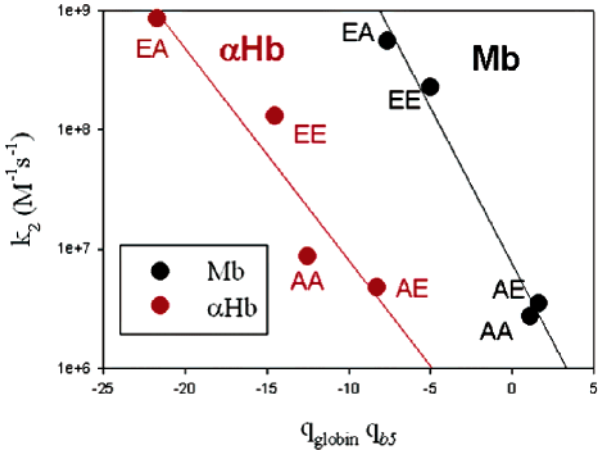

Figure 5. Logarithm of the bimolecular rate constant as a function of the charge product for the complexes of the [Mb/αHb, cyt b_5] reactivity "squares" at pH 7.0, 10 mM KPi.

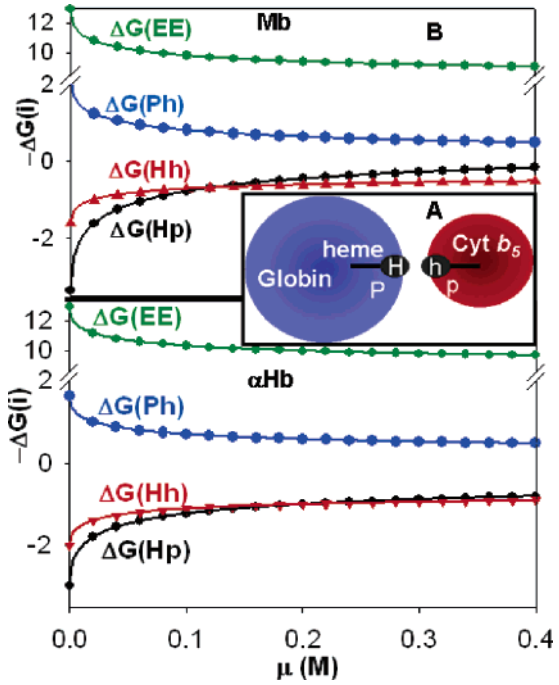

Figure 6. Ionic strength dependence of the electrostatic components of the free energy contributions, as defined in eqs 7−9 for Mb (upper) and α-Hb (lower). (*Inset*) Cartoon of the complex showing the local electrostatic contributions to reactive complex formation: heme−heme repulsion (Hh), heme−polypeptide interactions (Hp and Ph).

of reactive conformations (eq 3) defines an average free energy of binding for a reactive conformation, ΔG^R.

$$\ln k_2 = \ln(n_R k_R K_R) = \ln(n_R k_R) + \ln K_R$$
$$= \ln(n_R k_R) - \Delta G^R/RT \qquad (5)$$

It is not possible to use eq 5 to determine ΔG^R for a particular ET complex (e.g., **EA**) because it is combined with the unknown quantity $\ln(n_R k_R)$, but it is possible to decompose ΔG^R into individual contributions associated with heme−heme and heme−protein interactions and to determine these contributions. The analysis requires that heme neutralization does not perturb the proteins and changes only the binding constant of a reactive configuration and not its reactivity, thus leaving the term $\ln(n_R k_R)$ invariant.[9,11] This assumption is supported by the X-ray structure of ZnMb-dme presented above, which indeed shows that heme neutralization does not perturb the protein structure. Furthermore, neutralization does not change k^R through a change in the energetics of ET, for it has been shown that heme neutralization causes minimal changes in the heme reduction potential.[46,53−55]

The decomposition proceeds as follows. As illustrated in the cartoon of a bound complex presented in Figure 6, one may partition ΔG^R for the **AA** complex into four free-energy contributions, three of which are dominated by electrostatic interactions that involve the heme propionates:

$$\Delta G^R(\mathrm{AA}) = \Delta G^R(\mathrm{Pp}) + \Delta G^R(\mathrm{Hp}) + \Delta G^R(\mathrm{Ph}) + \Delta G^R(\mathrm{Hh}) \qquad (6)$$

(*i*) the interactions between the heme propionates of Mb/αHb (H) and the propionates of the cyt b_5 (h), which are denoted Hh interactions; (*ii*) those of the Mb/αHb heme propionates with the cyt b_5 polypeptide surface charges (p), denoted Hp; (*iii*) the interactions of the cyt b_5 propionates with the charges (P) on the Mb/αHb protein surface, denoted Ph; (*iv*) those between the polypeptides themselves, denoted Pp. Neutralization of one heme will eliminate the two electrostatic interactions between it and the partner protein while as a first approximation causing minimal changes in the remaining terms. As a result, the rate constants (eq 5) for a heme-neutralization square can be written in terms of these individual contributions to ΔG^R, plus an effective free energy for the **EE** complex, ΔG^{EE}, defined for convenience following our earlier introduction of such effective free energies in discussions of ET rate constants,[11]

$$-RT\ln(k_{2(\mathrm{EE})}) \equiv \Delta G^{EE} \equiv -RT\ln(n_R k_R) + \Delta G^R(\mathrm{Pp})$$
$$-RT\ln(k_{2(\mathrm{AA})}) = \Delta G^{EE} + \Delta G^R(\mathrm{Hp}) + \Delta G^R(\mathrm{Ph}) + \Delta G^R(\mathrm{Hh}) \qquad (7)$$

$$-RT\ln(k_{2(\mathrm{AE})}) = \Delta G^{EE} + \Delta G^R(\mathrm{Hp})$$
$$-RT\ln(k_{2(\mathrm{EA})}) = \Delta G^{EE} + \Delta G^R(\mathrm{Ph}) \qquad (8)$$

The use of eqs 6−8 immediately shows why heme neutralization is not symmetric. Neutralization of the Mb heme changes the binding free energy by eliminating $\Delta G^R(\mathrm{Hh}) + \Delta G^R(\mathrm{Hp})$, whereas for neutralization of the cyt b_5 heme eliminates $\Delta G^R(\mathrm{Hh}) + \Delta G^R(\mathrm{Ph})$. Only if the heme−heme repulsions dominated the interactions between the hemes and the peptides of their partners would there be approximate symmetry.

Through use of eq 8 we can estimate the individual free energy contributions associated with the interactions of the hemes from the four rate constants associated with the heme-

(52) Steinfeld, J. I.; Francisco, J. S.; Hase, W. L. *Chemical Kinetics and Dynamics*; Prentice Hall, Inc.: Englewood Cliffs, NJ, 1989.
(53) Rivera, M.; Seetharaman, R.; Girdhar, D.; Wirtz, M.; Zhang, X.; Wang, X.; White, S. *Biochemistry* **1998**, *37*, 1485−1494.
(54) Hunter, C. L.; Lloyd, E.; Eltis, L. D.; Rafferty, S. P.; Lee, H.; Smith, M.; Mauk, A. G. *Biochemistry* **1997**, *36*, 1010−1017.
(55) Eltis, L. D.; Herbert, R. G.; Barker, P. D.; Mauk, A. G.; Northrup, S. H. *Biochemistry* **1991**, *30*, 3663−3674.

Table 4. Free Energy (ΔG) for Each of the Interactions at μ = 0.02 and 0.4 M, pH 7.0

	ΔG(ab) [Mb] kcal/mol		ΔG(ab) [αHb] kcal/mol	
μ	0.02 M	0.4 M	0.02 M	0.4 M
ΔG(EE)	−10.8	−9.0	−11.1	−9.6
ΔG(Ph)	−0.92	−0.36	−1.0	−0.47
ΔG(Hp)	+1.62	+0.16	+1.79	+0.80
ΔG(Hh)	+1.01	−0.51	+1.40	−0.90

neutralization "square" of Scheme 1, which is equivalent to taking the ratios of rate constants:

$$\Delta G(\mathrm{Ph}) = -RT \ln(k_{2(\mathrm{EA})}/k_{2(\mathrm{EE})})$$

$$\Delta G(\mathrm{Hp}) = -RT \ln(k_{2(\mathrm{AE})}/k_{2(\mathrm{EE})})$$

$$\Delta G(\mathrm{Hh}) = -RT \ln([k_{2(\mathrm{AA})}k_{2(\mathrm{EE})}]/[k_{2(\mathrm{AE})}k_{2(\mathrm{EA})}]) \quad (9)$$

Table 4 presents the individual electrostatic free energies calculated in this manner for the measurements at low ionic strength (18 mM). We have also performed this decomposition as a function of ionic strength, and the results are presented in Figure 6.

If the reactive (R) conformations of the complex involve the heme of one protein coming in contact, or near-contact, with the heme of its partner at low ionic strength, one would expect a repulsion between the negatively charged heme propionates of Mb/αHb and the negative charges of the cyt b_5 polypeptide, particularly those near the cyt b_5 heme edge. This expectation is borne out by the analysis: ΔG(Hp) = +1.62 kcal/mol (Mb), +1.79 kcal/mol (αHb).

The free energy of interaction between the propionates of the two hemes (ΔG(Hh)) should likewise be unfavorable, and large, as the hemes come together (or nearly so) in a reactive complex. However, while the ΔG(Hh) is unfavorable as expected, it is *not* large and does not dominate the other terms. It is roughly two-thirds that of the heme-cyt b_5 polypeptide interaction for Mb (Hp) and a slightly larger fraction of the ΔG(Hp) for αHb: ΔG(Hh) = +1.01 kcal/mol (Mb), +1.40 kcal/mol(αHb).

One would instead expect the free energy for the interaction between the Mb/αHb polypeptide and that of cyt b_5 to be moderately favorable, as the Mb/αHb polypeptides both have slightly positive charges and cyt b_5 has a large, negative charge. This matches the decomposition: ΔG(Ph) = −0.92 kcal/mol (Mb), −1.0 kcal/mol (αHb).

The individual contributions to the free energy of reactive binding have been calculated over the range of ionic strengths, Figure 6;[56] the values for μ = 0.4 M are included in Table 4. For Mb, the high ionic strength nearly eliminates *each* contribution: each of the three heme interaction free energies decreases to an average of ∼0.3 kcal/mol at μ = 400 mM. The free energy contributions for αHb likewise become roughly equal but are significantly greater than the Mb values at the high ionic strength, averaging ∼0.7 kcal/mol. The strong dependence of ΔG_i on ionic strength verifies that the individual free energies of interaction are indeed electrostatic, thereby verifying the assumptions that lead to eqs 7−9.

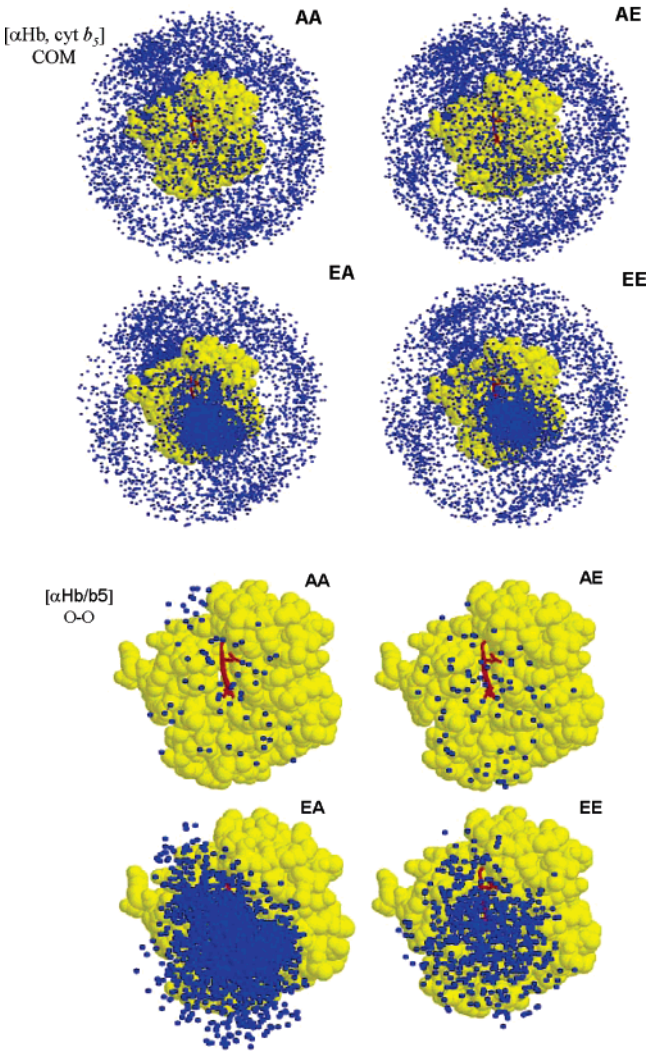

Figure 7. Docking profiles of the [αHb, cyt b_5] reactivity "square" from Brownian dynamics simulations. α-Chains are yellow, with hemes shown in red and directed toward the viewer. The blue dots are BD "hits", represented as the COM of cyt b_5. (Upper) COM criteria. (Lower) O−O criteria.

Brownian Dynamics Simulations. BD docking simulations were carried out for each of the [Mb/αHb, cyt b_5] complexes with two different docking criteria. (*i*) To examine the effects of heme neutralization on *binding* between the partners, we defined a "hit" to have occurred when the center-of-mass (COM) of the cyt b_5 comes within 39 Å of the COM of the Mb/αHb, the sum of the effective spherical radii of the component proteins plus the length of a hydrogen bond. (*ii*) To examine *reactive* docking, we defined a hit to have occurred when any of the four oxygen atoms of the heme propionate carboxylates of cyt b_5 approach to within 4 Å of one of the heme propionate oxygen atoms on Mb/αHb (O ⇔ O); the distance was arbitrarily chosen as being just larger than the length of a hydrogen bond.[57] Simulations with each criteria for the [αHb, cyt b_5] "square" are provided in Figure 7; simulations for the [Mb, cyt b_5] square are provided in the Supporting Information (Figure S5). The

(56) The dependences on *m* of these individual interaction free energies are well fit by a DH equation, analogous to eq 6, but where the derived charge product for a particular free energy contribution is fit in place of k_2 (Supporting Information). These DH fits are displayed to guide the eye but will not be discussed here.

(57) Kavanaugh, J. S.; Rogers, P. H.; Arnone, A. *Biochemistry* **2005**, *44*, 6101−6121.

Table 5. Number of Successful Hits from Brownian Dynamics Simulations

	Mb			αHb		
	O⟷O	COM	O⟷O/COM	O⟷O	COM	O⟷O/COM
AA	107	4207	0.025	67	4882	0.014
EA	2051	4595	0.446	1980	5348	0.370
AE	7	4170	0.002	76	4827	0.016
EE	532	4616	0.115	590	5198	0.114

number of successful hits under the two criteria are presented in Table 5; as the results for the Mb/αHb complexes are similar, we discuss only the αHb square. Comparison of the BD simulations for the four "corners" of the neutralization square, performed with the two reaction criteria, provides a visual illustration of the DD interaction between the two proteins.

The COM simulation for the **AA** combination of αHb with cyt b_5 (Figure 7) shows an approximately uniform distribution of hits over the αHb surface and *no* concentration of hits at the reactive αHb heme edge. None of the neutralizations, **EA**, **AE**, or **EE**, appreciably changes the number of COM hits (Table 5), although it does redistribute them, increasing the density of hits near the heme edge.

With the O ⟺ O criterion, the hits for all four complexes necessarily are close to the heme edge, and there are far fewer hits. For **AA**, comparison of the number of hits in the two simulations suggests that only ∼1−2% of all COM hits have O ⟺ O contacts that are likely to result in ET (Table 5). Neutralization of the αHb propionates in the **EA** complex causes a roughly 30-fold increase in the number of hits obtained with the O ⟺ O criteria, paralleling the $\sim 10^2$-fold increase in k_2 upon neutralization to form **EA** (Figure 7, Table 5); comparing the two criteria, now, ∼40% of the COM hits have O ⟺ O contacts that are likely to result in ET. In short, binding, as measured by the number of COM hits, changes little with neutralization and is indeed decoupled from reactivity as measured by the number of O ⟺ O hits. In contrast, **AE** has essentially the same number of reactive hits as **AA**, measured with the O ⟺ O criteria. while the number of O ⟺ O hits for the **EE** complex is *reduced* by approximately one-third. Both of these results also parallel the slight decreases in k_2 going from **EA** to **EE** for αHb.

Discussion

The DD binding/reactivity paradigm, in which many bound conformers contribute comparably to net binding but only a small fraction are reactive (eqs 1−3), was developed to explain the decoupling between ET reactivity and protein−protein binding observed in heme-neutralization studies (**AA** and **EA**) of ET between Mb and cyt b_5. The structural data presented here for ZnMb-dme confirms the assumption on which these studies rest: neither Zn substitution nor heme neutralization significantly alters a protein's structure.

ET pathways computations[11] suggest that a reactive conformer must have one or more of the propionates of the partner hemes in close proximity. Thus, we anticipated that the electrostatic repulsions between partner propionates would destabilize the few, but critically important, reactive conformers and that neutralizing *either* heme would enhance reactivity. To test this assumption we completed the "square" of heme-neutralized complexes (Scheme 1) by studying ET within the **AA**, **EA**, **AE**, and **EE** complexes of Mb and αHb. This assumption predicts that the **AE**, **EA**, and **EE** complexes all should show comparable increases in k_2 (eq 3). We were further alert, however, to the possibility that neutralization of both hemes by esterification, **EE**, might introduce hydrophobic attractions between the added methyl groups on the propionate partners that could enhance reactive binding.[3,58] However, our results reveal a different picture. Neutralization of Mb/αHb (**EA**) increases the bimolecular rate constant by $\sim 10^2$-fold, but neutralization of cyt b_5 (**AE**) has little effect on reactivity. Further neutralization of the second partner heme, which can have no beneficial influence on heme−heme repulsions, in fact causes a substantial decrease in k_2 if one compares **EE** to **EA** (k_2(**EE**) ≈ $^1/_2 k_2$(**EA**), whereas it causes a substantial increase in k_2 if one compares **EE** to **AE** (k_2(**EE**) ≈ $10k_2$(**AE**)). Clearly the electrostatic binding free energy that determines the K_R in eq 3 for the reactive **AA** complexes is *not* simply dominated by repulsions between the partner-heme propionates, as is required for heme neutralization to be "symmetric"! To interpret these measurements we have developed a simple approach (eqs 7−9) that allows us to quantify the contributions from three types of local electrostatic interactions to the average binding free energy of the reactive complexes (Figure 6, inset): heme−heme (Hh), Mb/αHb polypeptide−heme (Ph), and heme-cyt b_5 polypeptide (Hp) interactions.

In the following subsections, we first remark on the properties of the complex between the αHb complex and cyt b_5. Then we discuss the implications of the BD simulations for the interpretations of our findings for the heme-neutralization square. Next, we discuss the local contributions to the free energies of reactive binding that have been obtained from the heme-neutralization "squares" through use of eqs 7−9. Finally, we note possible implications of these results for the microscopic details of reactive binding in the [αHb/Mb, cyt b_5] complexes.

ET with αHb. Earlier, we had studied ET in the **AA** and **EA** complexes of cyt b_5 with αHb incorporated in the Hb tetramer.[15] These measurements also showed DD behavior: a large enhancement in reactivity at pH 7 upon heme neutralization of αHb ($\sim 10^2$), without a significant increase in affinity. In the present study we have employed monomeric αHb for simplicity. This is justified because αHb as the monomer and as incorporated in the Hb tetramer exhibits the same reactivity with cyt b_5; it is desirable because the monomer shows simplified ET kinetics. At pH 7, αHb is like Mb in that binding to cyt b_5 is sufficiently weak that saturation kinetics are not observed, only bimolecular kinetics. The logarithmic dependences of k_2 at pH 7 on the protein−protein charge products of the heme-neutralized "square" (Figure 5) confirm that the reactive binding of cyt b_5 to αHb, as well as Mb, can be understood within the DD model, as simply described by eq 3.

Interestingly, as seen in Table 1, binding of cyt b_5 to αHb becomes strong enough at pH 6.5 that saturation kinetics are observed, and in this case the decoupling of binding and reactivity is substantially suppressed. This suggests that an ET complex can perhaps be shifted between the DD and paradigms by manipulating the affinity either through changes in solvent conditions or through mutagenic design.

(58) Tsai, C. J.; Lin, S. L.; Wolfson, H. J.; Nussinov, R. *Protein science: a publication of the Protein Society* **1997**, *6*, 53−64.

Adapting BD Simulations to Probe DD. BD simulations of the reactions for the heme neutralization squares provide a graphic illustration of the central principle of DD, namely the decoupling of binding and reactivity. If no individual bound conformation (or subset) dominates the thermodynamic affinity constant, according to eq 2, then binding should be reflected in the total number of hits in a BD simulation when the COM criterion is employed. Those simulations give virtually the same number of hits for all members of a [Mb/αHb, cyt b_5] heme-neutralization square, Table 5, which clearly supports the idea that the overall binding is unchanged by neutralization of either or both hemes. In contrast, following eqs 2 and 3, the reactivity of a heme-neutralized complex relative to the **AA** complex, k/k_{et}, should be reflected in the binding of the reactive conformations alone, which is represented by the number of hits obtained in a simulation with the O ⇔ O criterion. In fact, the variations in the number of O ⇔ O hits for a neutralization square accurately reflect the variations of k_2. Overall, the BD simulations show that binding, as measured by COM hits, is indeed decoupled from reactivity as measured by the number of O ⇔ O hits.

Individual Contribution to the Free Energy of Reactive Binding. In the DD model as simply described by eqs 2 and 3, the observed second-order ET rate constant is proportional to the binding constant for reactive conformations. Therefore the logarithmic dependences of k_2 on the protein−protein charge products of the heme-neutralized "square" at pH 7 (Figure 5) confirm that the global electrostatic interactions contributed to the free energy of reactive binding. Nonetheless, the ET rate constants cannot be understood in terms of the binding between two charged species with particular net (global) charges. If that were so, then the **AE** complex of αHb would have the same k_2 as the **EA** complex of Mb, for the charge products of these two complexes are the same, using either of the definitions of charge product given above. Instead, however, $k_{2(EA)}$ for Mb is nearly 2 orders of magnitude greater than $k_{2(AE)}$ for αHb. The inference to be drawn is that interaction between *local* charges are controlling.

This recognition led us to develop a protocol for assessing the significance of local interactions by estimating the individual contributions to the free energy of reactive binding through measurement of the ET rate constants for the heme-neutralization "squares" of the [Mb/αHb, cyt b_5] complexes and their analysis with eqs 7−9. Table 4 contains the values for the low ionic strength interaction free energies of the heme−heme interactions (Hh), the Mb/αHb polypeptide−cyt b_5 heme interaction (Ph), and the Mb/αHb heme−cyt b_5 polypeptide interaction (Hp) (Figure 3A); the free energy of the **EE** complex includes an effective contribution associated with the rate constant (eq 7) and cannot be decomposed further.

The positive signs of ΔG(Hh) and ΔG(Hp) are in accord with simple intuition: ΔG(Hh) represents the heme−heme repulsions, and ΔG(Hp) represents the repulsion between the αHb/Mb heme propionates and the negatively charged cyt b_5 polypeptide. Likewise, ΔG(Ph) is negative, as expected because it represents the attractions of the cyt b_5 propionates to the positively charged polypeptide chains of Mb/αHb. However, the *magnitudes* of these three interaction energies are surprising: all are nearly the same, $\Delta G(\text{Hh}) \approx \Delta G(\text{Ph}) \lesssim \Delta G(\text{Hp})$ (∼0.4 kcal/mol greater). Focusing on ΔG(Hh), for the ET matrix element to be large enough to support the measured ET rates, one or more propionates of the partner hemes must be in very close proximity. Such a configuration would be energetically quite unfavorable and the estimated ΔG(Hh) seems far too low in magnitude for this. This assessment, of course, is based on the assumption that the distribution of reactive configurations is well represented by the average values for the binding free energies, but the assumption seems quite plausible. The strong distance dependence of the ET rate constant constitutes a "filter" which gives assurance that only those conformations with proximate propionates can be a "reactive" configuration.[9,11]

Speculation on the Microenvironment of the Complex Interface. The low magnitude of the heme−heme interaction free energy in reactive configurations calculated with eqs 7−9, $\Delta G(\text{Hh}) \approx 1$ kcal/mol at $\mu = 18$ mM, raises the following question: how can an effective ET pathway be established while circumventing the large free-energy penalty that would be paid for bringing the negatively charged carboxylates into close proximity? We discuss here three plausible answers.

The first possibility is that the propionates do not come in contact and that they are bridged by one or more ordered water molecules H-bonded to the carboxylates, and to each other if more than one water is involved. Recently, Lin et al.[59] simulated cyt b_5 self-exchange and found that a small number of structured waters bridging the carboxylates may actually enhance ET rates. In their simulations, they show that the electrostatic and van der Waals interactions between water and protein surfaces increases the probability of generating these water-molecule configurations that provide a large coupling between the two cyt b_5's. This kind of solvent-separated ET has been proposed for cross-linked azurin complexes,[60] peptidylglycine α-amidylating monooxygenase,[61] cytochrome c_2, and the photosynthetic reaction center.[62]

As a second possibility, the formation of a reactive complex might involve protonation of a propionate, thereby eliminating the repulsion entirely. In this case the interprotein ET pathway could involve the strong $-CH_2-COO^{-}\cdots H^{+}\cdots {}^{-}OOC-CH_2-$ symmetrical H-bond, whose formation could partly offset the protonation free energy, or it could involve the protonation plus additional intervening ordered waters, or even an ordered-water pathway in parallel.

There is a third possibility that can be viewed as a variant of the second. It is suggested by the observation that one propionate of both Mb and αHb is H-bonded to the side chain of residue 45 of each, neutralizing its negative charge; this residue is lysine in Mb and histidine in αHb. The formation of an ET pathway involving the H-bonded propionate of Mb/αHb and a propionate of cyt b_5 again would not pay a large propionate repulsion penalty. By suggesting that residue 45 may be of central importance in establishing an ET pathway, this further suggests tests by mutagenesis.

Summary

We have confirmed the basis of the heme-neutralization "square" approach with a crystal structure which shows that

(59) Lin, J.; Balabin, I. A.; Beratan, D. N. *Science* **2005**, *310*, 1311−1313.
(60) van Amsterdam, I. M. C.; Ubbink, M.; Einsle, O.; Messerschmidt, A.; Merli, A.; Cavazzini, D.; Rossi, G. L.; Canters, G. W. *Nat. Struct. Biol.* **2002**, *9*, 48−52.
(61) Francisco, W. A.; Wille, G.; Smith, A. J.; Merkler, D. J.; Klinman, J. P. *J. Am. Chem. Soc.* **2004**, *126*, 13168−13169.
(62) Miyashita, O.; Okamura, M. Y.; Onuchic, J. N. *Proc. Natl. Acad. Sci. U.S.A.* **2005**, *102*, 3558−3563.

heme neutralization causes negligible perturbation to the Mb structure. We have further shown that ZnαHb, like ZnMb, reacts with cyt b_5 on a DD energy landscape. Building on this foundation, we have measured the ET reactions with the [Mb/Hb, cyt b_5] heme-neutralization "squares" as a function of ionic strength. These studies verified that reactive binding of these complexes is strongly dependent on local electrostatic interactions and not merely upon the global electrostatic interaction characterized by the charge products of the reactive proteins. They further showed that the naive assumption of symmetrical changes upon neutralization of the heme of either partner is invalid. To analyze our findings we developed a method for decomposing the free energy of reactive binding into individual local electrostatic contributions, those of each heme with its partner protein's surface and that between the two hemes. This decomposition explains why the effects of heme neutralization are not symmetric: the magnitude of the heme−heme interaction free energy derived with this decomposition is low, $\Delta G(\mathrm{Hh}) \approx 1$ kcal/mol. This led us to consider three ways in which an effective ET pathway might be established between the propionates of the partner hemes yet circumvent the large free-energy penalty that would be paid if negatively charged carboxylates were to come into contact. Further theoretical and experimental studies will test the decomposition scheme proposed here, the assumptions that underpin it, and the speculations we have considered as possible explanations for the surprisingly low free energy for the heme−heme interaction.

Acknowledgment. This work was supported by the National Institutes of Health (HL62303). We thank the staff at the APS GM/CA-CAT beamlines for assistance with data collection and acknowledge the Keck Biophysics Facility at Northwestern University [http://www.biochem.northwestern.edu/Keck/keck-main.html.] for use of the Jasco CD spectrometer.

Supporting Information Available: Crystallographic parameters (Table S1), electrostatic properties (Table S2), circular dichroism spectra and thermal stability measurements (Figure S1), electrostatic potential surfaces (Figure S2), time-resolved triplet decay traces (Figure S3), ionic strength dependence of the bimolecular quenching rate constant (Figure S4), docking profiles from Brownian Dynamics simulations (Figure S5), experimental details for Brownian Dynamics simulations, and equations for analysis of binding titrations (Equation S1). This material is available free of charge via the Internet at http://pubs.acs.org.

JA067598G